



## Wet-Chemical Treatment of Si<sub>3</sub>N<sub>4</sub> Surfaces Studied Using Infrared Attenuated Total Reflection Spectroscopy

V. M. Bermudez<sup>z</sup>

Naval Research Laboratory, Electronics Science and Technology Division, Washington DC 20375-5347, USA

Infrared attenuated total reflection spectroscopy has been used to observe the surface chemistry of Si<sub>3</sub>N<sub>4</sub> films (grown on Si by low-pressure chemical vapor deposition) under steady-state conditions during exposure to dilute aqueous HF solutions. Surfaces etched in HF do not exhibit rapid growth of an SiO<sub>2</sub> layer when subsequently exposed to either humid room air at room temperature or to liquid H<sub>2</sub>O. However, some evidence is found for the formation of an ultrathin oxide-like layer when the etched surface is rinsed in deionized H<sub>2</sub>O. Removal of this layer in HF results in no detectable signal in the Si-H stretching region, unlike the case for Si subjected to a similar oxide-removal treatment. The presence of SiOH groups has been detected by observing their removal by reaction with aqueous acetic acid or HCl solutions, which suggests that SiH<sub>x</sub> groups are rapidly hydrolyzed. An attempt was made to detect surface NH<sub>x</sub> groups by protonation in aqueous acid to form NH<sub>x+1</sub><sup>+</sup>, which should be more readily observable in the infrared spectrum. However, the surface coverage of NH<sub>x</sub>, if any, is too small to be detected by this means. © 2005 The Electrochemical Society. [DOI: 10.1149/1.1851056] All rights reserved.

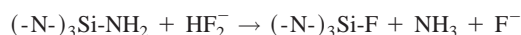
Manuscript submitted March 11, 2004; revised manuscript received August 5, 2004. Available electronically January 12, 2005.

Silicon nitride (Si<sub>3</sub>N<sub>4</sub>) is important as a dielectric material<sup>1</sup> for use in electronic devices, including ion-sensitive field-effect transistors (ISFETs). For these applications, thin films are often grown by chemical vapor deposition (CVD) or by sputter deposition. In contrast to the situation for many other electronic materials, little is known of a fundamental nature about the mechanisms involved in the wet-chemical processing (*e.g.*, cleaning, etching, surface passivation, etc.) of Si<sub>3</sub>N<sub>4</sub> films.

Previous studies<sup>2-7</sup> of the wet-chemical treatment of Si<sub>3</sub>N<sub>4</sub> films have focused primarily on etching in aqueous hydrofluoric acid (HF). The etch rate at room temperature for Si<sub>3</sub>N<sub>4</sub> grown by low-pressure chemical vapor deposition (LPCVD) is<sup>2</sup>  $R(\text{Å/s}) = 0.16[\text{HF}] + 0.31[\text{HF}_2^-]$  (where [X] is the molar concentration of species X) and is considerably slower than for material grown by plasma-enhanced chemical vapor deposition (PECVD). Knotter and Denteneer<sup>5</sup> proposed a mechanism for the etch rate dependence on pH in which, for the approximate range of  $1 < \text{pH} < 4.5$ , the rate-limiting step is



while at somewhat higher pH it is



A subsequent nucleophilic attack by F<sup>-</sup> at the Si<sup>δ+</sup>-F<sup>δ-</sup> site is then relatively rapid. Bower *et al.*<sup>8</sup> studied the cleaning of PECVD films and found that a modified RCA clean, followed by dipping in 1% HF, is effective in promoting subsequent wafer bonding, possibly as a result of the surface being terminated in amine (NH<sub>x</sub>) species.

Regrowth of the native oxide<sup>9-12</sup> (in air, in wet or dry O<sub>2</sub>, or in liquid H<sub>2</sub>O) on the HF-etched surface at room temperature is an important aspect of wet-chemical treatment and subsequent processing. Previous studies of LPCVD<sup>9,10</sup> or PECVD<sup>11</sup> Si<sub>3</sub>N<sub>4</sub> have found that surface oxidation at or somewhat above room temperature occurs readily in room air and in H<sub>2</sub>O vapor but more slowly in dry O<sub>2</sub>. A high concentration of N-H bonds, which occurs in PECVD material, is found<sup>11</sup> to increase the reaction rate with H<sub>2</sub>O. Hydrolysis<sup>10,11</sup> removes Si-H and NH<sub>x</sub> groups, produces SiO<sub>2</sub> with surface SiOH groups, and releases NH<sub>3</sub>. Ultrathin H-free Si<sub>3</sub>N<sub>4</sub> films grown on Si(111) by reaction at high-temperature with NH<sub>3</sub> under ultrahigh vacuum (UHV) conditions,<sup>12</sup> are found to resist dry O<sub>2</sub> oxidation at temperatures up to ~500°C, to an extent depending on the preparation of the Si substrate prior to nitridation. An unre-

solved issue, which may depend on the details of Si<sub>3</sub>N<sub>4</sub> growth and oxidation conditions, is whether the native oxide is better described as SiO<sub>2</sub> or as an oxynitride, possibly with a graded O/N ratio.

Results for the oxidation and/or hydrolysis of high-surface-area (HSA) Si<sub>3</sub>N<sub>4</sub> powders,<sup>13-15</sup> obtained using primarily infrared (IR) spectroscopy, concur with those noted above for thin films. The reaction with H<sub>2</sub>O vapor is more rapid than with dry O<sub>2</sub> and is accelerated by the presence of NH<sub>x</sub> groups. After removal of adsorbed H<sub>2</sub>O and other contaminants by evacuation at elevated temperature, (-N-)<sub>3</sub>SiOH and (-Si-)<sub>2</sub>NH are found<sup>16,17</sup> to be the dominant surface species. Other works,<sup>18-26</sup> reporting the interaction of HSA powders with liquid H<sub>2</sub>O and/or aqueous acids, are also relevant. When immersed in H<sub>2</sub>O at a pH of 7.0, HSA Si<sub>3</sub>N<sub>4</sub> shifts the pH either higher or lower, depending<sup>19</sup> on the relative surface concentrations of basic [Si-(NH)-Si and Si-NH<sub>2</sub>] or acidic [Si-OH] sites, and reversible hydrolysis of (-Si-)<sub>3</sub>N sites can alter the concentrations of such species.<sup>24</sup> In nonetching acidic solutions, amine and hydroxyl sites can undergo reversible protonation<sup>24,25</sup> to form Si-(NH<sub>2</sub><sup>+</sup>)-Si, Si-NH<sub>3</sub><sup>+</sup>, and Si-OH<sub>2</sub><sup>+</sup>.

In this work we are concerned with observing the surface chemistry of Si<sub>3</sub>N<sub>4</sub> under steady-state conditions during exposure to aqueous HF. The experimental technique used here is IR attenuated total reflectance (ATR) spectroscopy which has been used previously (*e.g.*, Ref. 27-29 and works cited therein) for *in situ* studies of the wet-chemical processing of Si. The present work is, to our knowledge, the first attempt to extend such experiments to Si<sub>3</sub>N<sub>4</sub>.

### Experimental

The samples were ~45 nm thick films of Si<sub>3</sub>N<sub>4</sub> grown by LPCVD on both sides of a Si substrate. Details concerning the growth, surface cleaning under UHV conditions and characterization of these samples are given elsewhere.<sup>30</sup> No cleaning of the as-received sample was done prior to mounting it in the flow cell (see below). The Si substrate was an internal reflection element (IRE), cut in an arbitrary crystallographic orientation, which was obtained commercially (Harrick Corporation, Ossining, NY). The IRE was a 25 × 15 × 1 mm<sup>3</sup> parallelepiped with a 60° internal reflection angle which gave a total of fourteen reflections at the two faces for light propagating parallel to the long edge. Of these, eleven reflections probed the fluid/sample interface (as opposed to the sealing surfaces of the cell). Following Queeney *et al.*,<sup>27</sup> the IRE geometry was chosen to reduce the intensity of the liquid H<sub>2</sub>O absorption bands (see below) and to extend the transmission range so that SiO<sub>2</sub> modes could be studied.

The Si<sub>3</sub>N<sub>4</sub>-coated IRE was mounted in a Teflon flow cell<sup>27-29</sup> with both sides in contact with the reagent fluid. The Teflon, which

<sup>z</sup> E-mail: bermudez@estd.nrl.navy.mil

was pressed tightly around the edges of the IRE to form a fluid-tight seal, contributed weak absorptions in ATR at 1152 and 1207  $\text{cm}^{-1}$ , and the transmission cutoff of the Si IRE occurred at about 980  $\text{cm}^{-1}$ . The cell was connected to a pumping system which permitted a continuous flow of fluid at room temperature and the changing of fluids without exposing the sample to air. The total cell volume was 5.3 mL, and the typical flow rate was  $\sim 20 \text{ mL min}^{-1}$ . Teflon and polyethylene were the only materials, other than Si or  $\text{Si}_3\text{N}_4$ , in contact with the reagents. The HF solution was prepared by successive dilutions, with deionized (DI)  $\text{H}_2\text{O}$ , of a standard concentrated solution, which is 49% by weight in  $\text{H}_2\text{O}$ . With a density of 1.19  $\text{g cm}^{-3}$ , 34.3 mL of the concentrate contains 1 mole of HF.

Spectroscopic data were recorded with a Mattson Cygnus 100 Fourier-transform IR system and a narrow-band  $\text{HgCd}_x\text{Te}_{1-x}$  detector at a resolution of 8  $\text{cm}^{-1}$  with 2000 scans averaged in about 10 min. The entire optical path was purged with dry  $\text{N}_2$ . Triangle apodization with fourfold zero filling was used in processing the interferograms. A spectrum recorded with pure DI  $\text{H}_2\text{O}$  flowing through the cell was used as a reference and the quantity  $\delta R/R$  obtained, where  $\delta R (\ll R)$  is the fractional change in reflectance caused by addition of the reagent of interest (*i.e.*,  $\delta R \equiv R_{\text{reagent}} - R_{\text{water}}$ ).

### Results and Discussion

**Preliminary considerations.**—Before proceeding to the data, a numerical simulation of the ATR experiment is considered. This is useful in evaluating the sensitivity to species on the  $\text{Si}_3\text{N}_4$  surface and in further analysis of the data. Calculations were done for a model system consisting of a Si substrate with a 45 nm thick  $\text{Si}_3\text{N}_4$  overlayer covered by an adsorbate layer in contact with an  $\text{H}_2\text{O}$  ambient. As in the experiment, light is incident internally at an angle of  $60^\circ$  at the IRE/fluid interface. The calculations were performed using the matrix formalism (fully described in Ref. 31<sup>a</sup>) for the polarized reflectance of a multilayer system with ideal interfaces between homogeneous and isotropic materials. Complex optical constants ( $n, k$ ) for liquid  $\text{H}_2\text{O}$  and for PECVD  $\text{Si}_3\text{N}_4$  were obtained as functions of  $h\nu$  from the literature (Ref. 32 and 33, respectively). For crystalline Si, the real index ( $n$ ) in the region of low absorption ( $h\nu > 1000 \text{ cm}^{-1}$ ) was obtained in the form of a Sellmeier function.<sup>34</sup> (Thus, the multiphonon absorptions above  $1000 \text{ cm}^{-1}$  were neglected.) For an  $\text{SiO}_2$  adsorbate layer, the optical constants of silica glass<sup>34</sup> were used. Methanol was also used as a model adsorbate because the IR oscillator parameters for the liquid are available<sup>35,b,36</sup> and because it exhibits absorptions that are reasonably close in energy to those expected for  $\text{SiH}_x$  and  $\text{NH}_x$  on the  $\text{Si}_3\text{N}_4$  surface (see below). The fact that an actual  $\text{CH}_3\text{OH}$  film would dissolve in  $\text{H}_2\text{O}$  is irrelevant since only the model optical constants are significant here.

Figure 1 shows  $R$  and  $\delta R/R$  for both s and p polarization, where  $\delta R$  is the difference in reflectance (see above) with and without a 0.5 nm thick layer of randomly oriented (*i.e.*, liquid)  $\text{CH}_3\text{OH}$  as a model adsorbate. Downward-pointing features are due to the  $\text{CH}_3\text{OH}$  layer, while upward-pointing structure arises from  $\text{H}_2\text{O}$ . The latter features appear in  $\delta R/R$  because the presence of the thin  $\text{CH}_3\text{OH}$  layer reduces accordingly the sampling depth into the  $\text{H}_2\text{O}$  ambient. Hence, when the  $\text{CH}_3\text{OH}$  is removed in the calculation of  $\delta R/R$ , the  $\text{H}_2\text{O}$  absorptions gain intensity and appear as positive features. The results illustrate the higher sensitivity in p polarization and also the difficulties imposed by the strong  $\text{H}_2\text{O}$  absorptions. For eleven internal reflections (see above), the estimated transmission for unpolarized light at the  $\sim 3400 \text{ cm}^{-1}$   $\text{H}_2\text{O}$  absorption maximum

<sup>a</sup> There is a typographical error in this edition that affects calculations of multilayer transmission. Equation 4.170 should read  $T = 1/S_{11}$ .

<sup>b</sup> There is a typographical error that affects the application of the formalism in this paper. The factor of  $4\pi/3$  in the numerator of Eq. 21b should be simply  $4\pi$ .

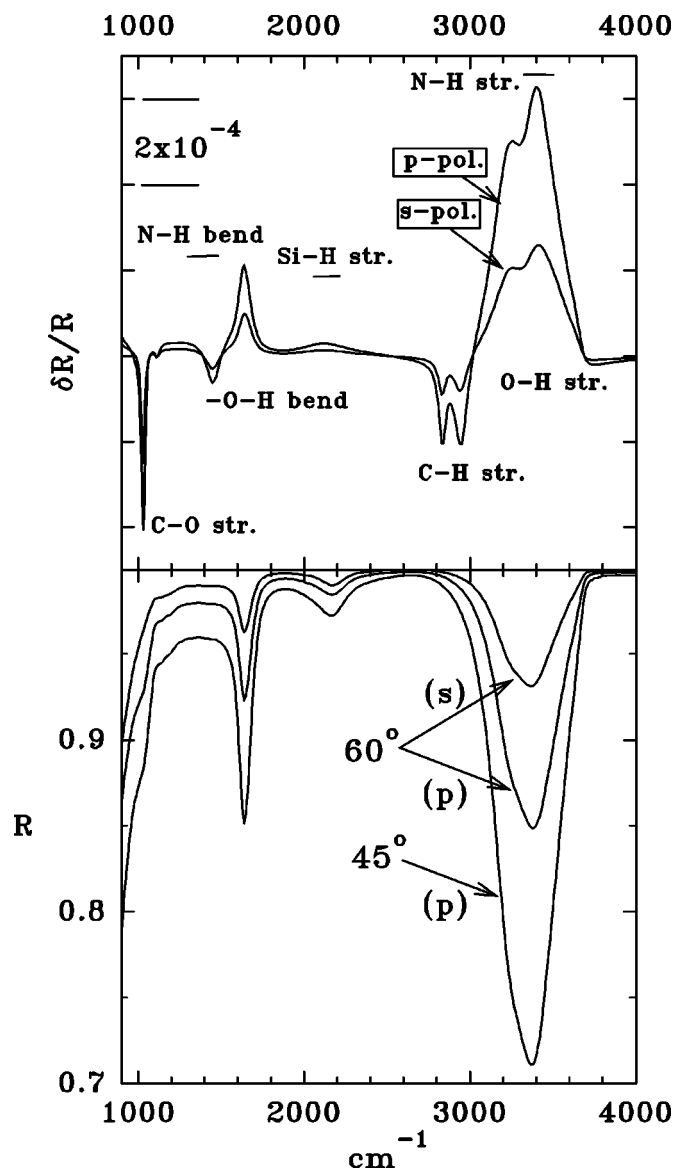


**Figure 1.** Results of model calculations for a Si IRE covered with a 45 nm thick  $\text{Si}_3\text{N}_4$  layer having a 0.5 nm thick film of  $\text{CH}_3\text{OH}$  on the surface in an  $\text{H}_2\text{O}$  ambient. (a) Shows  $\delta R/R$ , the fractional change in reflectance caused by addition of the  $\text{CH}_3\text{OH}$  film, in p and s polarization at an internal reflection angle of  $60^\circ$ . All peaks are stronger in p than in s polarization. (b) Shows the reflectance at  $60^\circ$  for p and s polarization and at  $45^\circ$  for p polarization. The various vibrational modes are labeled (str. = stretching), including the approximate regions expected for H on the  $\text{Si}_3\text{N}_4$  surface. The C-O, C-H and O-H modes are those of  $\text{H}_2\text{O}$  and/or  $\text{CH}_3\text{OH}$ . The magnitudes of  $R$  and  $\delta R/R$  pertain to a single internal reflection.

is 28% for a  $60^\circ$  angle of incidence. The situation is more favorable in the vicinity of the N-H bending modes, where the transmission at the  $1634 \text{ cm}^{-1}$  absorption peak is  $\sim 57\%$ . Similar results for  $\delta R/R$  at  $45^\circ$  (not shown) indicate an approximately fivefold higher sensitivity to adsorbates on the  $\text{Si}_3\text{N}_4$  surface, the combined effect of a larger  $\delta R/R$  per reflection and of a greater number of reflections for the same IRE length. However, the calculated  $R_p$  (Fig. 1b) shows that the sample would be effectively opaque in the regions surrounding the  $\text{H}_2\text{O}$  absorptions.

Turning now to the etching reagents, dilute HF solutions (typically about 0.01–0.02 M,  $\text{pH} \approx 2.7$ ) were employed so that the etch rate would be sufficiently slow that the  $\text{Si}_3\text{N}_4$  films would be useable for several experiments. There was no obvious dependence of

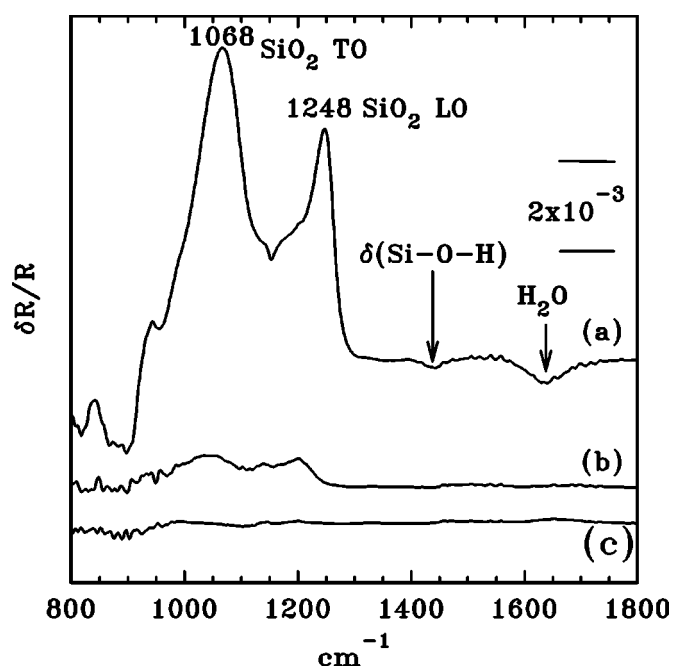


**Figure 2.** (a) Data in the region of  $\text{SiO}_2$  absorption for a bare Si IRE in contact with 0.02 M HF. The reference spectrum was obtained in pure  $\text{H}_2\text{O}$  before exposure to HF; hence, positive-going features represent species removed by the HF. The native oxide was formed by exposure of an HF-treated surface to humid room air at room temperature (see text). (b) Shows data, as in (a), for the initial exposure of an as-received  $\text{Si}_3\text{N}_4$  sample to the HF solution. (c) Shows a typical baseline obtained for two successive data sets with DI  $\text{H}_2\text{O}$  flowing in the cell. The traces have been displaced vertically for clarity. The sensitivity scale shows  $\delta R/R$  per reflection. The IR beam was p polarized. Note that the IRE transmission is effectively zero below  $980\text{ cm}^{-1}$ .

the data on the previous use of a sample (*i.e.*, on the number of prior experiments). Since, as noted above, the  $\text{Si}_3\text{N}_4$  surface chemistry can depend on the nature of the film growth, a check of the etch rate was done by recording a normal-incidence IR transmission spectrum (in a dry  $\text{N}_2$  ambient) for a  $\text{Si}_3\text{N}_4$ -coated Si sample before and after exposure to 0.087 M HF (pH  $\approx$  2.3). From the loss in the peak absorbance of the transverse optical (TO) phonon band, an etch rate of  $0.14\text{ nm min}^{-1}$  was deduced which is in good agreement with previous results<sup>2</sup> ( $0.17\text{ nm min}^{-1}$ ) for LPCVD  $\text{Si}_3\text{N}_4$ . Since it has been reported (see above) that HSA  $\text{Si}_3\text{N}_4$  powders are attacked by water, it was considered useful to determine whether the same might be true for the LPCVD films used here. A  $\text{Si}_3\text{N}_4$ -coated Si wafer was etched in aqueous HF to remove the oxide and then immersed in static DI  $\text{H}_2\text{O}$  at room temperature. Based again on the absorbance of the TO mode, no significant loss of  $\text{Si}_3\text{N}_4$  was seen after 43 h. This is consistent with the observation<sup>2</sup> that the LPCVD  $\text{Si}_3\text{N}_4$  etch rate in aqueous HF goes to zero with the concentrations of HF and  $\text{HF}_2^-$ .

**Infrared results.**—Figure 2a shows results for a bare Si IRE (one for which the  $\text{Si}_3\text{N}_4$  coating had been etched off) after exposure to humid room air<sup>c</sup> for four days to form a native oxide. The data provide a reference spectrum for an  $\text{SiO}_2$  film obtained under the present conditions. The spectrum was recorded *in situ* with p polarized radiation after etching off the oxide in flowing 0.02 M HF. Upward-pointing (positive) features represent species removed by the HF, while downward-pointing (negative) structure is due to spe-

cies that are added by the etching process. Removal of the oxide layer is evidenced by the peaks at  $1068$  and  $1248\text{ cm}^{-1}$  which correspond,<sup>27</sup> respectively, to the TO and longitudinal optical (LO) Si-O stretching modes of  $\text{SiO}_2$ . The additional weak structure at  $\sim 1154\text{ cm}^{-1}$  is due to a slight miscancellation of a Teflon absorption as noted above.

The weak feature at  $\sim 1438\text{ cm}^{-1}$  is tentatively assigned to the bending mode of surface Si-O-H groups, hydrogen-bonded to  $\text{H}_2\text{O}$ , on the basis of the appearance of the C-O-H bending mode at  $1452\text{ cm}^{-1}$  in liquid  $\text{CH}_3\text{OH}$  (cf. Fig. 1). However, it is noted that other studies<sup>27,37</sup> of wet-chemical growth or etching of oxides on Si have not reported this mode. The small peak at the  $1634\text{ cm}^{-1}$  liquid- $\text{H}_2\text{O}$  absorption, which also appears in the numerical simulations discussed above (cf. Fig. 1), arises from the fact that a slightly increased thickness of  $\text{H}_2\text{O}$  is sampled as the oxide layer is removed. Numerical simulation also indicates an oxide thickness of  $\sim 1.5\text{ nm}$  based on the peak height of the TO band. The TO mode was used for the thickness estimate since the peak intensity, unlike that of the LO mode,<sup>27</sup> is insensitive to the exact optical constants of the ambient liquid. These simulations were done as described above using  $\text{SiO}_2$ , rather than  $\text{CH}_3\text{OH}$ , as the surface film.

In contrast to these results, data for an as-received  $\text{Si}_3\text{N}_4$ -coated IRE (Fig. 2b) gave little or no indication of the removal of an  $\text{SiO}_2$  layer during the initial HF treatment. Figure 2b shows a spectrum recorded at the end of the  $\text{Si}_3\text{N}_4$  native oxide removal. Continued exposure to HF resulted only in the monotonic growth of a feature (see below) due to the thinning of the  $\text{Si}_3\text{N}_4$  film. Following removal of the oxide (if any) in HF, exposure to flowing DI  $\text{H}_2\text{O}$  for  $\sim 30$  min or to humid room air (overnight) did not result in the appearance of an  $\text{SiO}_2$  spectrum (Fig. 2a) in data obtained during subsequent exposure to HF. This indicates that rapid hydrolytic oxidation does not occur under the present conditions for the LPCVD films studied here. Previously such rapid oxidation was observed somewhat above room temperature for PECVD films,<sup>11</sup> at room temperature for HSA powders,<sup>13-15</sup> and for LPCVD films undergoing chemomechanical polishing.<sup>10</sup> The present results appear to be consistent with those of Raider *et al.*<sup>9</sup> who etched LPCVD  $\text{Si}_3\text{N}_4$  in HF and performed surface analysis, using X-ray photoemission spectroscopy, after exposure to room air. Rapid growth of 0.2-0.3 nm of oxide was seen, followed by only very slow growth beyond that point.

However, some evidence was found for the formation of an ultrathin oxide-like layer by hydrolysis of the HF-treated  $\text{Si}_3\text{N}_4$  surface during postetch rinsing in  $\text{H}_2\text{O}$ . Figure 3a shows data, obtained with a nominally unpolarized IR beam, for prolonged exposure to HF. Unpolarized radiation was used in order to reduce the relative intensity<sup>27</sup> of the  $\text{Si}_3\text{N}_4$  LO phonon absorption which peaks at about  $1130\text{ cm}^{-1}$  (Ref. 30) and contributes to the tail extending to  $\sim 1200\text{ cm}^{-1}$  in Fig. 3a. The peak at  $\sim 1000\text{ cm}^{-1}$  results from the tail of the TO phonon absorption, which peaks at  $804\text{ cm}^{-1}$  (Ref. 30), and the rapidly decreasing Si IRE transmission below  $1000\text{ cm}^{-1}$ . Its appearance in  $\delta R/R$  is due to the loss of  $\text{Si}_3\text{N}_4$  absorption as etching progresses. The data in Fig. 3b resulted when the etched surface was rinsed in DI  $\text{H}_2\text{O}$  and then briefly treated again with HF. The spectrum shows the change, relative to the rinsed surface, caused by the brief ( $\sim 10$  min) HF treatment. The  $\text{Si}_3\text{N}_4$  peak appears, due to the further etching of that material, together with a shoulder at about  $1125\text{ cm}^{-1}$  which is ascribed to the removal of a layer formed when the etched surface was exposed to pure  $\text{H}_2\text{O}$  (or to dissolved  $\text{O}_2$ ) during rinsing. Continued exposure to HF resulted in the further growth of the  $\text{Si}_3\text{N}_4$  peak but not of the shoulder. The shoulder was difficult to observe, and Fig. 3b shows the clearest of several data sets.

In view of the very weak absorption (cf. Fig. 2), this layer might better be described as an ultrathin oxide-like layer rather than as  $\text{SiO}_2$ . The exact assignment of the  $\sim 1125\text{ cm}^{-1}$  feature is uncertain. It is probably too high in energy to be ascribed to the Si-OH stretch

<sup>c</sup> The term humid room air means that the sample was rinsed with flowing DI  $\text{H}_2\text{O}$  to remove HF, after which the Teflon cell was drained and vented to room air. Water droplets retained in the lines to the pump are assumed to saturate the air in the cell.

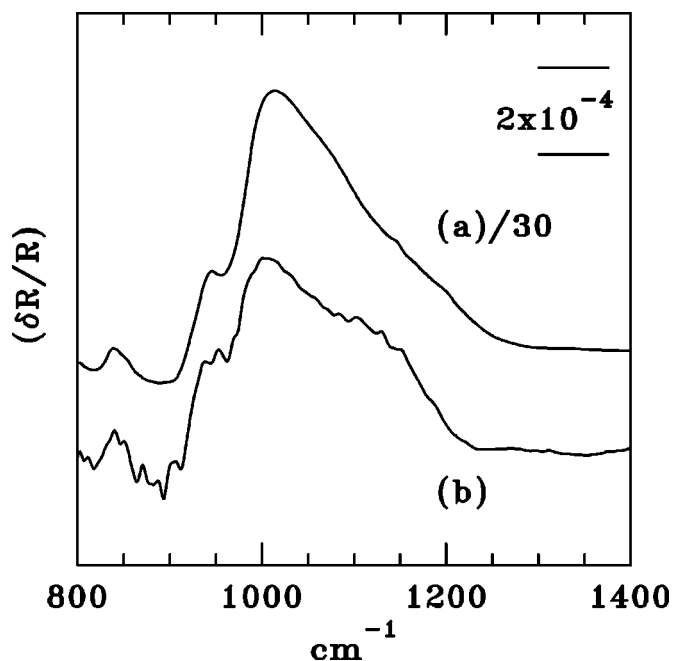


**Figure 3.** Data showing the hydrolysis of the HF-etched  $\text{Si}_3\text{N}_4$  surface. (a) Shows the spectrum after prolonged HF etching, referenced to the as-received surface in DI  $\text{H}_2\text{O}$ . The peak at  $\sim 1000\text{ cm}^{-1}$  is related to the removal of  $\text{Si}_3\text{N}_4$  (see text). (b) Shows data for this HF-etched surface after a  $\sim 30$  min rinse in flowing DI  $\text{H}_2\text{O}$ . The spectrum was obtained after exposing the  $\text{H}_2\text{O}$ -rinsed surface again to HF (referenced to the rinsed surface) and shows the removal of more  $\text{Si}_3\text{N}_4$  and of an oxygen species formed during the rinse. Trace (a) has been reduced in intensity by a factor of 30, relative to trace (b), and displaced vertically for clarity. The sensitivity scale shows  $\delta R/R$  per reflection. The IR beam was nominally unpolarized.

which, for isolated OH groups on a Si surface, appears<sup>38</sup> at  $840\text{ cm}^{-1}$ ; although, the frequency may be higher for a Si site multiply-coordinated to N, instead of to Si, due to the partial positive charge on Si bonded to N. It is noted that various Si-O-Si stretching modes are seen<sup>38</sup> in the  $990\text{--}1050\text{ cm}^{-1}$  range for Si(100) oxidized by  $\text{H}_2\text{O}$  vapor under UHV conditions. Hence, this mode might be due to an O bridging ( $-\text{N}-$ )<sub>3</sub>Si sites.

Evidence for the existence of SiOH groups is seen in Fig. 4a. Here the HF etching solution was rinsed out with 5% (by volume) of glacial acetic acid in  $\text{H}_2\text{O}$ , rather than with pure  $\text{H}_2\text{O}$ . Formic acid [ $\text{HOC}(=\text{O})\text{H}$ ] vapor has been found<sup>16</sup> to react with SiOH groups on HSA  $\text{Si}_3\text{N}_4$  powders to form the silyl ester [e.g.,  $(-\text{N}-)$ <sub>3</sub>Si-OC(=O)H]. The peak at  $3645\text{ cm}^{-1}$  is assigned to the removal<sup>d</sup> of isolated OH groups (*i.e.*, those not H-bonded to  $\text{H}_2\text{O}$ ). This mode is close in energy to that seen<sup>29</sup> on Si surfaces in contact with aqueous HF ( $3642\text{ cm}^{-1}$ ); however, for HSA  $\text{Si}_3\text{N}_4$  powders after high-temperature evacuation<sup>17</sup> the  $(-\text{N}-)$ <sub>3</sub>Si-O-H stretch appears at a somewhat higher energy,  $3717\text{ cm}^{-1}$ . The corresponding Si-O-H bending mode (cf. Fig. 2) was obscured by the edge of the strong acetic acid absorption at  $1392\text{ cm}^{-1}$ . The strong upward-pointing  $\text{H}_2\text{O}$  absorption band at  $\sim 3300\text{ cm}^{-1}$  appears because the acetic acid solution is more concentrated (*i.e.*, contains less  $\text{H}_2\text{O}$ ) than the HF reference solution. There will also be a contribution in this region<sup>29</sup> from the removal of any SiOH groups that are H-bonded to  $\text{H}_2\text{O}$ . Figure 4b shows a similar feature when the HF is displaced by a 0.3 M aqueous HCl solution (see below). In this case,

<sup>d</sup> The actual reaction product cannot be identified from the present data due to interference from strong absorptions in the acetic acid solution. The appearance of the SiO-H mode in  $\delta R/R$  means simply that the reaction has replaced the SiOH groups with another species not absorbing in the vicinity of  $3645\text{ cm}^{-1}$ .

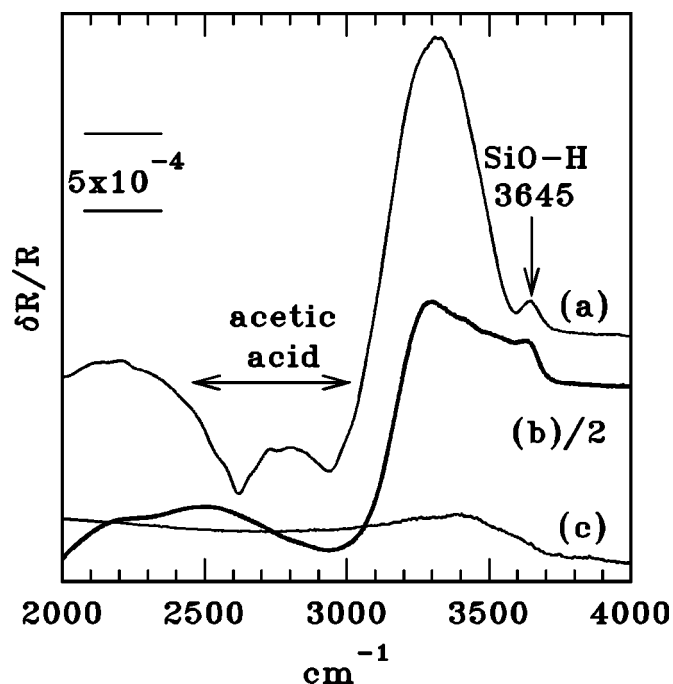


**Figure 4.** (a) Data obtained in p polarization showing the result of rinsing out the HF solution with a 5% (by volume) solution of glacial acetic acid in  $\text{H}_2\text{O}$ . The reference spectrum is that of the HF solution; hence, features pointing up (down) correspond to species removed (added) by the acetic acid. The structure in the  $2500\text{--}3000\text{ cm}^{-1}$  range arises from acetic acid C-H stretching modes. The sensitivity scale shows  $\delta R/R$  per reflection. (b) Similar to (a) but showing the effect of rinsing out the HF solution with 0.3 M HCl. The spectrum has been divided by a factor of two relative to (a). (c) Similar to (a) and (b) but showing the effect of rinsing out the HF with DI  $\text{H}_2\text{O}$ . The spectra have been displaced vertically for clarity.

the removal of the isolated SiOH arises from the conversion<sup>24,25</sup> of SiOH to  $\text{SiOH}_2^+$  in the strongly acidic HCl solution.

The reaction product is easily hydrolyzed since data obtained upon rinsing out the acetic acid or HCl solution with pure  $\text{H}_2\text{O}$  (not shown) indicate that the surface SiOH is reformed. However, when the HF is rinsed out with DI  $\text{H}_2\text{O}$  instead of an acid (Fig. 4c), no SiO-H peak is observed. It is also noted that no narrow IR absorption bands appear near this frequency for dilute aqueous HF solutions.<sup>39,40</sup> Furthermore, no additional structure was seen to indicate a similar interaction between acetic acid or HCl and surface  $\text{NH}_x$  species (see below).

It is useful to consider why SiOH appears in Fig. 4a,b but is not observed either during HF etching or after rinsing out the HF with pure  $\text{H}_2\text{O}$  (Fig. 4c). It has been proposed<sup>41</sup> that an acid attack on the SiOH group is the rate-limiting step in HF etching of  $\text{SiO}_2$ . If this process is slow for SiOH on the  $\text{Si}_3\text{N}_4$  surface then the steady-state coverage of SiOH in dilute HF would not be much less than that in pure  $\text{H}_2\text{O}$ . The SiOH signature in  $\delta R/R$  (dilute HF solution referenced to pure  $\text{H}_2\text{O}$ ) would then be weak, recalling that the experiment detects only differences in surface composition. On the other hand, if a large fraction of the SiOH is removed, for example, by esterification in acetic acid solution, then this loss would be detected in  $\delta R/R$ .

Figure 5 shows data in the Si-H stretching region for a bare Si IRE (*i.e.*, one with no nitride layer) and for a  $\text{Si}_3\text{N}_4$ -coated IRE, all recorded using nominally unpolarized radiation. For  $\text{Si}_3\text{N}_4$ , native oxide refers to a surface exposed to DI  $\text{H}_2\text{O}$  after etching in HF, as described above. No evidence is seen for the formation of  $\text{SiH}_x$  groups on the  $\text{Si}_3\text{N}_4$  surface following exposure to HF. The weak

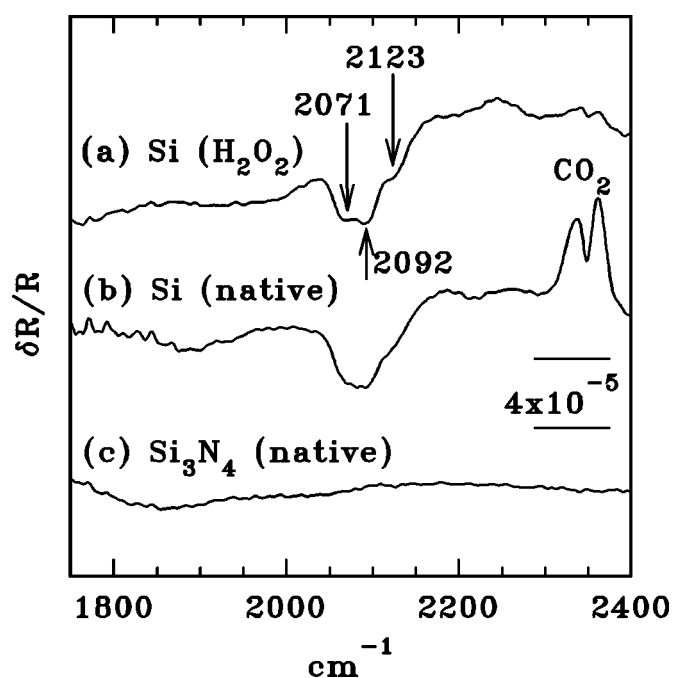


**Figure 5.** The Si-H stretching region for (a) a bare Si IRE after removal of an oxide layer formed in 15 wt %  $\text{H}_2\text{O}_2$  in  $\text{H}_2\text{O}$ , (b) a bare Si IRE after removal of the native oxide formed by exposure to laboratory air at room temperature and (c) a  $\text{Si}_3\text{N}_4$ -coated Si IRE after removal of the native oxide (see text). In all cases, the oxide was removed by exposure to a flowing 0.087 M HF solution. The sensitivity scale shows  $\Delta R/R$  per reflection, and the spectra have been displaced vertically for clarity. Trace (b) shows a small residual signal from atmospheric  $\text{CO}_2$  (and from  $\text{H}_2\text{O}$  vapor, below  $1850\text{ cm}^{-1}$ ) in the optical path. The IR beam was nominally unpolarized.

broad band at  $\sim 1850\text{ cm}^{-1}$  is a characteristic<sup>39,40</sup> of aqueous HF solutions.

For the bare IRE (Fig. 5b), removal of the native oxide in aqueous HF results in a clear Si-H signature<sup>28,42</sup> in the form of a broad band at  $\sim 2080\text{ cm}^{-1}$  with a shoulder at  $\sim 2115\text{ cm}^{-1}$ . This structure is somewhat better resolved after removal of an oxide grown by exposure<sup>29</sup> to 15 wt %  $\text{H}_2\text{O}_2$  in  $\text{H}_2\text{O}$ , with peaks appearing at about 2071 and 2092  $\text{cm}^{-1}$  and the shoulder at  $\sim 2123\text{ cm}^{-1}$ . Since the present Si surface is not crystallographically well-defined, no attempt is made to assign these features to specific  $\text{SiH}_x$  species.<sup>28,42</sup>

For  $\text{Si}_3\text{N}_4$ , the Si-H stretching modes would fall in the 2100–2300  $\text{cm}^{-1}$  range,<sup>43,44</sup> depending on the local environment of the Si atom (*i.e.*, on back-bonding to N vs. O). In the bulk of the film, an Si-H stretching mode, due to a small amount of H remaining from LPCVD growth, was seen<sup>30</sup> at  $2200\text{ cm}^{-1}$  by referencing the spectrum for a  $\text{Si}_3\text{N}_4$ -coated IRE to that of a bare IRE (all in a dry  $\text{N}_2$  ambient). However, no  $\text{SiH}_x$  is detectable on the chemically treated  $\text{Si}_3\text{N}_4$  surface under conditions for which it can be seen on elemental Si. This is true for the initial HF treatment of the as-received sample and for removal of either the native oxide or of an oxide formed, as above, by exposure to aqueous  $\text{H}_2\text{O}_2$ . In view of the evidence given above for the presence of surface  $\text{SiOH}$ , this result is consistent with the rapid hydrolysis of Si-H sites on the  $\text{Si}_3\text{N}_4$  surface, as noted elsewhere.<sup>11,13,17</sup>

Proceeding now to the question of surface amine sites, Table I summarizes the reported<sup>45–56</sup> mode frequencies for various  $\text{NH}_x^+$  and  $\text{NH}_x$  species. The  $\text{NH}_x^+$  values were obtained from IR and Raman data for crystalline salts containing methyl- or ethylammonium cations, and the  $\text{NH}_x$  data are from IR spectra of aminosilanes. It is noted that the  $\nu(\text{N-H})$  modes for  $\text{NH}_x^+$  are lower in energy than those of the neutral  $\text{NH}_x$  species and generally lie below the region of

**Table I.** Vibrational frequencies ( $\text{cm}^{-1}$ ) for  $\text{NH}_x^+$  and  $\text{NH}_x$  groups.<sup>a</sup>

	$\nu_a$	$\nu_s$	$\delta_1$	$\delta_2$
$\text{CH}_3\text{NH}_3^+$ <sup>b</sup>	3080–3231	2993–3159	1578–1632	1534–1575
$(\text{CH}_3)_2\text{NH}_2^+$ <sup>c</sup>	3049–3233	3034–3216	1536–1574	1433–1444
$(\text{CH}_3)_3\text{NH}^+$ <sup>d</sup>		2760	1215	
$\text{R}_3\text{Si-NH}_2$ <sup>e</sup>	3474–3483	3401–3405	1536–1552	
$(\text{R}_3\text{Si})_2\text{NH}$ <sup>f</sup>		3351–3382	1164–1179	

<sup>a</sup>  $\nu_a$  = antisymmetric stretch;  $\nu_s$  = symmetric stretch;  $\delta_{1,2}$  = deformation. The description of  $\delta_{1,2}$  as bending, scissoring, rocking, or wagging varies for different studies and depends on the chemical species. Other deformations, which fall below  $900\text{ cm}^{-1}$ , have been omitted.

<sup>b</sup> Reference 45–47. The values given represent the ranges reported in different studies for various compounds.

<sup>c</sup> Reference 48–52. The values given represent the ranges reported in different studies for various compounds.

<sup>d</sup> Reference 53. The data are for  $[(\text{CH}_3)_3\text{NH}]_2\text{SiF}_6$  in which strong  $-\text{N-H}^+\text{-F}^-$  hydrogen bonding shifts  $\nu_s$  to a low value. For  $[(\text{C}_2\text{H}_5)_3\text{NH}]\text{SbCl}_6$ , Ref. 54,  $\nu_s = 2703\text{ cm}^{-1}$  with ( $3164\text{ cm}^{-1}$  without)  $\text{NH}^+\text{-Cl}^-$  hydrogen bonding.

<sup>e</sup> Reference 55, 56; R = alkyl group. For HSA  $\text{Si}_3\text{N}_4$  following evacuation at high temperature, the corresponding frequencies for this species are reported (Ref. 17) to be 3510, 3450, and  $1550\text{ cm}^{-1}$ .

<sup>f</sup> Reference 55. For HSA  $\text{Si}_3\text{N}_4$  following evacuation at high temperature, the corresponding frequencies for this species are reported (Ref. 17) to be 3350 and  $1470\text{ cm}^{-1}$ .

strong  $\text{H}_2\text{O}$  absorption (cf. Fig. 1). Hence,  $\text{NH}_x^+$  species should be observable if the  $\nu(\text{N-H})$  bands are sufficiently intense. For a 0.01–0.02 M HF solution ( $\text{pH} \approx 2.7$ ) the results of Knotter and Denteneer<sup>5</sup> suggest that any surface  $\text{NH}_x$  sites should be protonated; hence,  $\text{NH}_x^+$  species are more likely than the neutral analogs. In the bulk of the film an N-H stretching mode due to H remaining from LPCVD growth was seen,<sup>30</sup> as described above, at  $3335\text{ cm}^{-1}$ .

Observation of the  $\text{NH}_x$  or  $\text{NH}_x^+$  bending modes under the present conditions is difficult due to interference from the strong  $\text{H}_2\text{O}$  absorption (cf. Fig. 1) and from the additional effect of a slight miscancellation of the Si multiphonon absorptions in the 1250–1500  $\text{cm}^{-1}$  range. The latter effect could be eliminated by the use of a Ge IRE. Although thick ( $0.3\text{ }\mu\text{m}$ )  $\text{Si}_3\text{N}_4$  films have been grown<sup>57</sup> on Ge by PECVD, Ge has not to our knowledge been evaluated as a substrate for the growth of thin films (such as those used here) by LPCVD which requires a higher substrate temperature than does PECVD.

An attempt was made to observe  $\text{NH}_x$  species by taking advantage of the protonation-induced shift in  $\nu(\text{N-H})$  noted above. Data were taken while flowing a 0.3 M HCl solution through the cell (after having displaced the dilute HF solution). The HCl was used to increase the  $\text{H}_3\text{O}^+$  concentration without incurring the higher etch rate that would result from a concentrated HF solution. No  $\text{NH}_x^+$  signatures were observed (Fig. 4b) in the  $2700\text{--}3200\text{ cm}^{-1}$  range (cf. Table I) above the  $\Delta R/R$  detection limit of  $\sim 1 \times 10^{-5}$  per reflection. The same is true in the absence of HCl, *i.e.*, for a dilute HF etching solution. In  $\text{H}_2\text{O}$  solution, both HCl and HF give broad absorption bands, with somewhat different structure,<sup>39</sup> in the  $\sim 2500\text{--}3700\text{ cm}^{-1}$  range which contribute to  $\Delta R/R$  in Fig. 4b.

This null result suggests that, under steady-state conditions in dilute aqueous HF,  $(-\text{N}-)_3\text{SiOH}$  (probably H-bonded to  $\text{H}_2\text{O}$ ) is the dominant surface species and that the attack on  $\text{NH}_x^+$  sites is too rapid to permit formation of a sufficiently high concentration of these species to be detectable in the present experiment. A further implication is that the rate-limiting step under these conditions may be an attack on the Si-N back bond at the  $(-\text{N}-)_3\text{SiOH}$  site. It is difficult to estimate how low the relative  $\text{NH}_x^+$  surface coverage would have to be in order to be undetectable. However, IR data for

HSA powders<sup>16,17</sup> show that the integrated intensity for the (-Si-)N-H stretching mode is considerably greater than that of the (-N-)SiO-H mode. Assuming that the coverages of the two species are about the same on the HSA powders *in vacuo* then, based on the present  $\delta R/R$  detection limit and on the observed SiO-H intensity (Fig. 4a,b), a conservative estimate indicates that the  $\text{NH}_x^+$  coverage would have to be at least a factor five lower than that of SiOH in order to escape detection. This upper limit estimate is further reduced if one recalls that the SiO-H band in Fig. 4a,b reflects only the fraction of SiOH sites not H-bonded to  $\text{H}_2\text{O}$ .

### Conclusions

Infrared attenuated total reflection spectroscopy has been used to observe the surface chemistry of  $\text{Si}_3\text{N}_4$  films under steady-state conditions during exposure to dilute aqueous HF solutions. Surfaces etched in HF do not exhibit rapid growth of an  $\text{SiO}_2$  layer when subsequently exposed to either humid room air at room temperature or to liquid  $\text{H}_2\text{O}$ . However, some evidence is found for the formation of an ultrathin oxide-like layer when the etched surface is rinsed in deionized  $\text{H}_2\text{O}$ . Removal of this layer in HF results in no detectable signal in the Si-H stretching region, unlike the case for Si subjected to a similar oxide-removal treatment. However, surface SiOH is observed via reaction with acetic acid or HCl solution, suggesting that  $\text{SiH}_x$  sites on the  $\text{Si}_3\text{N}_4$  surface are rapidly hydrolyzed. Protonation of surface  $\text{NH}_x$ , to form  $\text{NH}_{x+1}^+$  sites, should shift the  $\nu(\text{N-H})$  stretching modes to lower energy and away from the region of strong  $\text{H}_2\text{O}$  absorption. However, no  $\text{NH}_x$  was detectable by this means which indicates a low steady-state coverage.

These results have implications for chemical processes aimed at the functionalization of (*i.e.*, the attachment of organic ligands to)  $\text{Si}_3\text{N}_4$  surfaces following exposure to aqueous HF treatment, since they suggest SiOH, and not  $\text{SiH}_x$  or  $\text{NH}_x$ , as the reactive species remaining after such treatment. In this context, it is noted that several groups have reported the functionalization of HF-treated  $\text{Si}_3\text{N}_4$  surfaces using alkyl bromides<sup>58</sup> or alkyl chlorosilanes.<sup>59-61</sup> In analogy with  $\text{SiO}_2$  surfaces,<sup>62</sup> these reactions could occur at SiOH sites on the  $\text{Si}_3\text{N}_4$  surface, via elimination of HBr or HCl, or even by direct attack at strained Si-N-Si bridges. One study<sup>63</sup> reported reaction with 1-alkenes (*i.e.*,  $\text{H}_2\text{C} = \text{CH-R}$ , where R is a long-chain *n*-alkyl ligand) which almost certainly involves surface  $\text{SiH}_x$  sites.<sup>64</sup> However, the  $\text{Si}_3\text{N}_4$  used in that work was thought to be Si-rich with, possibly, a surface chemistry more like that of pure Si than of  $\text{Si}_3\text{N}_4$ .

### Acknowledgments

This work was supported by the Office of Naval Research. F. K. Perkins is thanked for helpful discussions leading to the inception of this work and for obtaining the ATR samples. A. E. Berry is thanked for helpful discussions, and M. Klanjsek Gunde kindly provided the  $\text{Si}_3\text{N}_4$  optical constants in digital form.

Naval Research Laboratory assisted in meeting the publication costs of this article.

### References

- F. H. P. M. Habraken and A. E. T. Kuiper, *Mater. Sci. Eng., R.*, **12**, 123 (1994).
- C. A. Deckert, *J. Electrochem. Soc.*, **127**, 2433 (1980); *J. Electrochem. Soc.*, **125**, 320 (1978).
- K. Domanský, D. Petelenz, and J. Janata, *Appl. Phys. Lett.*, **60**, 2074 (1992).
- V. K. Rathi, M. Gupta, and O. P. Agnihotri, *Microelectron. J.*, **26**, 563 (1995).
- D. M. Knotter and T. J. J. Denteneer, *J. Electrochem. Soc.*, **148**, F43 (2001).
- G. C. Han, P. Luo, K. B. Li, Z. Y. Liu, and Y. H. Wu, *Appl. Phys. A: Solids Surf.*, **74**, 243 (2002).
- K. B. Sundaram, R. E. Sah, H. Baumann, K. Balachandran, and R. M. Todi, *Microelectron. Eng.*, **70**, 109 (2003).
- R. W. Bower, M. S. Ismail, and B. E. Roberds, *Appl. Phys. Lett.*, **62**, 3485 (1993).
- S. I. Raider, R. Flitsch, J. A. Aboaf, and W. A. Pliskin, *J. Electrochem. Soc.*, **123**, 560 (1976).
- Y. Z. Hu, R. J. Gutmann, and T. P. Chow, *J. Electrochem. Soc.*, **145**, 3919 (1998).
- J. N. Chiang, S. G. Ghanayem, and D. W. Hess, *Chem. Mater.*, **1**, 194 (1989).
- R. M. Wallace and Y. Wei, *J. Vac. Sci. Technol. B*, **17**, 970 (1999).
- P. Ho, R. J. Buss, and R. E. Loehman, *J. Mater. Res.*, **4**, 873 (1989).
- Y.-L. Li, Y. Liang, F. Zheng, K. Xiao, Z.-Q. Hu, and T. Shun, *J. Mater. Sci. Lett.*, **14**, 713 (1995).
- J. Szépvölgyi, I. Mohai, and J. Gubicza, *J. Mater. Chem.*, **11**, 859 (2001).
- G. Busca, V. Lorenzelli, G. Porcile, M. I. Baraton, P. Quintard, and R. Marchand, *Mater. Chem. Phys.*, **14**, 123 (1986).
- G. Ramis, G. Busca, V. Lorenzelli, M. I. Baraton, T. Merle-Mejean, and P. Quintard, in *Surfaces and Interfaces of Ceramic Materials*, L.-C. Dufour, C. Monty, and G. Petot-Ervas, Editors, p. 173, Kluwer, Dordrecht (1989).
- L. Bergström and R. J. Pugh, *J. Am. Ceram. Soc.*, **72**, 103 (1989).
- P. Greil, *Mater. Sci. Eng., A*, **109**, 27 (1989).
- L. Bergström and E. Bostedt, *Colloid Surf.*, **49**, 183 (1990).
- M. Kulig and P. Greil, *J. Mater. Sci.*, **26**, 216 (1991).
- S. G. Malghan, *Colloid Surf.*, **62**, 87 (1992).
- V. A. Hackley and S. G. Malghan, *J. Mater. Sci.*, **29**, 4420 (1994).
- S. Mezzasalma and D. Baldovino, *J. Colloid Interface Sci.*, **180**, 413 (1996).
- C. Galassi, F. Bertoni, S. Ardizzone, and C. L. Bianchi, *J. Mater. Res.*, **15**, 155 (2000).
- E. Laarz, B. V. Zhmud, and L. Bergström, *J. Am. Ceram. Soc.*, **83**, 2394 (2000).
- K. T. Queeney, H. Fukidome, E. E. Chaban, and Y. J. Chabal, *J. Phys. Chem. B*, **105**, 3903 (2001).
- M. Niwano, *Surf. Sci.*, **427-428**, 199 (1999).
- S. Watanabe, *Surf. Sci.*, **341**, 304 (1995).
- V. M. Bermudez and F. K. Perkins, *Appl. Surf. Sci.*, **235**, 406 (2004).
- R. M. A. Azzam and N. M. Bashara, *Ellipsometry and Polarized Light*, Chap. 4, North-Holland, Amsterdam (1977).
- J. E. Bertie and Z. Lan, *Appl. Spectrosc.*, **50**, 1047 (1996). See <http://www.ualberta.ca/~jbertie/JEBHOME.HTM> for (*n*, *k*) of  $\text{H}_2\text{O}$  in digital form.
- M. Klanjsek Gunde and M. Macek, *Phys. Status Solidi A*, **183**, 439 (2001).
- Handbook of Optical Constants of Solids*, Vol. 1, E. D. Palik, Editor, Academic Press, Orlando, FL (1985).
- J. E. Bertie, S. L. Zhang, and C. D. Keefe, *J. Mol. Struct.*, **324**, 157 (1994).
- J. E. Bertie and Z. Lan, *J. Chem. Phys.*, **105**, 8502 (1996).
- S. Fujimura, K. Ishikawa, and H. Ogawa, *J. Vac. Sci. Technol. A*, **16**, 375 (1998).
- M. K. Weldon, B. B. Stefanov, K. Raghavachari, and Y. J. Chabal, *Phys. Rev. Lett.*, **79**, 2851 (1997).
- P. A. Giguère and S. Turrell, *J. Am. Chem. Soc.*, **102**, 5473 (1980).
- J. Khorami, R. Beaudoin, and H. Ménard, *Can. J. Chem.*, **65**, 817 (1987).
- D. M. Knotter, *J. Am. Chem. Soc.*, **122**, 4345 (2000).
- Y. Sugita and S. Watanabe, *Jpn. J. Appl. Phys., Part 1*, **37**, 3272 (1998).
- A. D. Bailey III and R. A. Gottscho, *Jpn. J. Appl. Phys., Part 1*, **34**, 2172 (1995).
- E. Bustarret, M. Bensouda, M. C. Habrard, J. C. Bruyère, S. Poulin, and S. C. Gujrathi, *Phys. Rev. B*, **38**, 8171 (1988).
- D. Zeroka and J. O. Jensen, *J. Mol. Struct.*, **425**, 181 (1998).
- B. L. George, I. H. Joe, and G. Aruldas, *J. Raman Spectrosc.*, **23**, 417 (1992).
- H. Jeghno, A. Ouasri, M. Elyoubi, A. Rhandour, M.-C. Dhamelincourt, P. Dhamelincourt, and A. Mazzah, *J. Raman Spectrosc.*, **35**, 261 (2004).
- V. P. Mahadevan Pillai, V. U. Nayar, and V. N. Jordanovska, *Spectrochim. Acta, Part A*, **56**, 887 (2000).
- M. B. Smirnov, I. S. Ignat'ev, V. Yu. Kazimirov, and L. A. Shuvalov, *Kristallografiya*, **44**, 103 (1999); English transl.: *Crystallogr. Rep.*, **44**, 98 (1999).
- G. Bator, R. Jakubas, J. Lefebvre, and Y. Guinet, *Vib. Spectrosc.*, **18**, 203 (1998).
- Th. Zeegers-Huyskens and G. Bator, *Vib. Spectrosc.*, **13**, 41 (1996).
- G. Bator, J. Baran, R. Jakubas, and H. Ratajczak, *Vib. Spectrosc.*, **6**, 193 (1994).
- A. Ouasri, A. Rhandour, M.-C. Dhamelincourt, P. Dhamelincourt, and A. Mazzah, *Spectrochim. Acta, Part A*, **59**, 851 (2003).
- B. Bednarska-Bolek, Z. Ciunik, R. Jakubas, G. Bator, and P. Ciapała, *J. Phys. Chem. Solids*, **63**, 507 (2002).
- A. Marchand, M.-T. Forel, F. Metras, and J. Valade, *J. Chim. Phys.*, **61**, 343 (1964).
- J. Plazanet, F. Metras, A. Marchand, and J. Valade, *Bull. Soc. Chim. Fr.*, **1967**, 1920.
- R. Kishore, S. N. Singh, and B. K. Das, *Infrared Phys. Technol.*, **38**, 83 (1997).
- F. Cattaruzza, A. Cricenti, A. Flamini, M. Girasole, G. Longo, A. Mezzi, and T. Prospero, *J. Mater. Chem.*, **14**, 1461 (2004).
- T. Ito, M. Namba, P. Bühlmann, and Y. Umezawa, *Langmuir*, **13**, 4323 (1997).
- M. M. Sung, G. J. Kluth, and R. Maboudian, *J. Vac. Sci. Technol. A*, **17**, 540 (1999).
- J. E. Headrick and C. L. Berrie, *Langmuir*, **20**, 4124 (2004).
- T. Yasuda, M. Nishizawa, S. Yamasaki, and K. Tanaka, *J. Vac. Sci. Technol. B*, **18**, 1752 (2000).
- A. Arafat, K. Schroën, L. C. P. M. de Smet, E. J. R. Sudhölter, and H. Zuilhof, *J. Am. Chem. Soc.*, **126**, 8600 (2004).
- J. M. Buriak, *Chem. Rev. (Washington, D.C.)*, **102**, 1272 (2002).